SLAC-PUB-15823

Novel QCD Phenomena and New Perspectives for Hadron Physics

Stanley J. Brodsky[1]

[1]*SLAC National Accelerator Laboratory*
Stanford University, Stanford, California 94309, USA

I discuss novel aspects of hadron structure and dynamics derived from the light-front quantization of QCD. These include: (a) the nonperturbative origin of intrinsic heavy quarks in the nucleon at large x; the modification of pQCD factorization theorems due to the lensing corrections from initial- and final-state interactions; (b) important corrections to pQCD scaling for inclusive reactions due to processes in which hadrons are created directly at high transverse momentum in hard processes and their relation to the baryon anomaly in high-centrality heavy-ion collisions; and (c) the nonuniversality of quark distributions in nuclei. I also discuss some novel theoretical perspectives in QCD: (a) light-front holography – a relativistic color-confining first approximation to QCD based on the AdS/CFT correspondence principle; (b) the principle of maximum conformality – a method which determines the renormalization scale at finite order in perturbation theory, yielding scheme independent results; (c) the replacement of quark and gluon vacuum condensates by "in-hadron condensates" and how this helps to resolves the conflict between the QCD vacuum and the cosmological constant.

I. INTRODUCTION

In this contribution to the proceedings of the International Workshop on Low-x Physics, I will review a number of unexpected phenomenological features of quantum chromodynamics, including:

- The novel effects arising from the multiply-connected heavy-quark quantum fluctuations of hadron wavefunctions;
- Corrections to pQCD leading-twist scaling for inclusive reactions due to processes in which hadrons are created at high transverse momentum directly in the hard process;
- The anomalous baryon to meson ratio seen at high transverse momentum in heavy ion collisions at RHIC;
- The indications that antishadowing is flavor-dependent; and
- The modification of factorization theorems from the "lensing" corrections due to initial and final state interactions; and the non-universality of quark distributions in nuclei

I will also briefly discuss some novel theoretical perspectives in QCD:

- Light-front holography – a first approximation to QCD based on the AdS/CFT correspondence principle;
- The principle of maximum conformality – which determines the renormalization scale order-by-order in perturbation theory yielding scheme-independent results; and
- How to resolve the apparent conflict between the physics of the QCD vacuum and the cosmological constant.

Additional discussion of some of the novel features of QCD discussed here may be found in my recently published Annual Review of Nuclear and Particle Science article with Marek Karliner and Guy de Teramond, ref. [1].

II. HADRON PHYSICS ON THE LIGHT FRONT

The quantization of QCD at fixed light-front (LF) time $\tau = t + z/c$ – light-front quantization – provides a first-principles method for solving nonperturbative QCD. Given the Lagrangian, one can compute the LF Hamiltonian H_{LF} in terms of the independent quark and gluon fields. The eigenvalues of H_{LF} determine the mass-squared values of both the discrete and continuum hadronic spectra. The eigensolutions $|\Psi_H\rangle$ projected on the free n-parton Fock state $\langle n|\Psi_H\rangle$ determine the LF wavefunctions $\psi_{n/H}(x_i, \vec{k}_{\perp i}, \lambda_i)$ where the $x_i = \frac{k_i^+}{P^+} = \frac{k_i^0+k_i^3}{P^0+P^3}$, with $\sum_{i=1}^n x_i = 1$,

Work supported in part by US Department of Energy under contract DE-AC02-76SF00515.

are the light-front moment fractions. The eigenstates are defined at fixed $\tau = x^+$ within the causal horizon, so that causality is maintained without normal-ordering. In fact, light-front physics is a fully relativistic field theory, but its structure is similar to non-relativistic atomic physics, and the resulting bound-state equations can be formulated as relativistic Schrödinger-like equations at equal light-front time.

A remarkable feature of LFWFs is the fact that they are frame independent; i.e., the form of the LFWF is independent of the hadron's total momentum $P^+ = P^0 + P^3$ and $P_\perp$. The boost invariance of LFWFs contrasts dramatically with the complexity of boosting the wavefunctions defined at fixed time t. [2] Light-front quantization is thus the ideal framework to describe the structure of hadrons in terms of quark and gluon constituents. The constituents' angular momentum properties of the hadrons are also encoded in the LFWFs. The total angular momentum projection [3] $J^z = \sum_{i=1}^n S_i^z + \sum_{i=1}^{n-1} L_i^z$ is conserved Fock-state by Fock-state and by every interaction in the LF Hamiltonian. The constituent spin and orbital angular momentum properties of the hadrons are thus encoded in their LFWFs. The empirical observation that quarks carry only a fraction of the nucleon angular momentum highlights the importance of quark orbital angular momentum. In fact the nucleon anomalous moment and the Pauli form factor are zero unless the quarks carry nonzero L^z.

Light-Front quantized field theory in physical $3+1$ space-time has a holographic dual with the dynamics of theories in five-dimensional anti-de Sitter (AdS) space [4], giving important insight into the nature of color confinement in QCD. Light-front holography – the duality between the front form and classical gravity based on the isometries of AdS_5 space, provides a new method for determining the eigenstates of the QCD LF Hamiltonian in the strongly coupled regime. In the case of mesons, for example, the valence Fock-state wavefunctions of H_{LF} for zero quark mass satisfy a single-variable relativistic equation of motion in the invariant variable $\zeta^2 = b_\perp^2 x(1-x)$, which is the impact variable related to the constituent's invariant mass squared $M^2_{q\bar{q}}$. The effective confining potential $U(\zeta^2)$ in this frame-independent "light-front Schrödinger equation" systematically incorporates the effects of higher quark and gluon Fock states [5]. The hadron mass scale – its "mass gap" – is generated in a novel way. Remarkably, the potential $U(\zeta^2)$ has a unique form of a harmonic oscillator potential if one requires that the chiral QCD action remains conformally invariant [5, 6]. The result is a nonperturbative relativistic light-front quantum mechanical wave equation which incorporates color confinement and other essential spectroscopic and dynamical features of hadron physics.

Given the frame-independent light-front wavefunctions (LFWFs) $\psi_{n/H}$, one can compute a large range of hadronic observables, starting with form factors, structure functions, generalized parton distributions, Wigner distributions, etc. For example, the "handbag" contribution [7] to the E and H generalized parton distributions for deeply virtual Compton scattering can be computed from the overlap of LFWFs, automatically satisfy the known sum rules. One can calculate the electromagnetic and gravitational form factors $< p+q|j^\mu(0)|p >$ and $< p+q|t^{\mu\nu}(0)|p >$ of a hadron from the Drell-Yan-West formula – i.e., the overlap of LFWFs. The anomalous gravitomagnetic moment $B(0)$ defined from the spin-flip matrix element $< p+q|t^{\mu\nu}(0)|p >$ at $q \to 0$ vanishes – consistent with the equivalence theorem of gravity. In contrast, in the instant form, the overlap of instant time wavefunctions is not sufficient. One must also couple the photon probe to currents arising spontaneously from the vacuum which are connected to the hadron's constituents. In the case of deep-inelastic lepton-proton scattering $\ell p \to \ell' X$ the lepton scatters at fixed x^+ on any quark in any one of the proton's Fock states. The higher Fock states of a proton such as $|uudQ\bar{Q}\rangle$ are the source of the sea-quark distributions, including contributions "intrinsic" to the proton structure [8]. One can also analyze and prove factorization and evolution equations for exclusive processes [9–11]. Analogous light-front methods can be applied to inclusive process where more than one parton from an initial- or final-state hadron are involved such as the Drell-Yan process at high x_F [12].

A measurement in the front form is analogous to taking a flash picture. The image in the resulting photograph records the state of the object as the front of the light wave from the flash illuminates it; in effect, this is a measurement within the spacelike causal horizon ${\Delta x_\mu}^2 \leq 0$. Similarly, measurements such as deep inelastic lepton-hadron scattering $\ell H \to \ell' X$, determine the LF wavefunctions and structure of the target hadron H at fixed light-front time. For example, the BFKL Regge behavior of structure functions can be demonstrated [13] from the behavior of LFWFs at small x. The interactions of the struck quark on the spectators quarks in the final state produce "lensing effects" such as the pseudo-T-odd. 'Sivers' effect [14], the correlation $\vec{S} \cdot \vec{q} \times \vec{p}_q$ of the proton polarization with the virtual photon-quark scattering plane which is Such lensing effects are leading twist; i.e. they are not power-law suppressed [15]. The Sivers correlation from initial-state lensing in the Drell-Yan process has the opposite sign [16–18]. The lensing interactions can be considered as properties of the LFWFs augmented by a Wilson line [19]. The existence of "lensing effects" at leading twist, such as the T-odd "Sivers effect" in spin-dependent semi-inclusive deep-inelastic scattering, was first demonstrated using LF methods [15].

The physics of diffractive deep inelastic scattering and other hard processes where the projectile hadron remains intact, such as $\gamma^* p \to X + p'$, is also most easily analysed using LF QCD [20]. LF quantization thus provides a discriminant [21] between static (the square of LFWFs) distributions versus non-universal dynamic structure functions, such as the diffractive deep inelastic scattering and Sivers effect which involve final-state interactions. The nuclear shadowing and flavor-dependent anti-shadowing also arise [22]. Other QCD properties such as "color transparency" [23],

the "hidden color" of the deuteron LFWF [24], and the existence of intrinsic heavy quarks in the LFWFs of light hadrons [8, 25] can be derived from the structure of hadronic LFWFs. It is also possible to compute jet hadronization at the amplitude level from first principles from the LFWFs [26].

Hadron observables, e.g., hadronic structure functions, form factors, distribution amplitudes, GPDs, TMDs, and Wigner distributions can be computed as simple convolutions of light-front wavefunctions (LFWFs). The Light-Front method is directly applicable for describing atomic bound states in both the relativistic and nonrelativistic domains; it is particularly useful for atoms in flight since the LFWFs are frame-independent. It also satisfies theorems such as cluster decomposition.

III. INTRINSIC HEAVY QUARKS

If one follows conventional wisdom, nonvalence "sea " quarks are produced only from gluon splitting; i.e., the proton only contains valence quarks and gluons at an initial soft scale. and DGLAP evolution from the $g \to Q\bar{Q}$ spitting process generates all of the sea quarks at $Q^2 > 4m_Q^2$. If this was correct, then the $\bar{u}(x)$ and $\bar{d}(x)$ antiquark distributions in the proton would be identical. This hypothesis also predicts that the $s(x)$and $\bar{s}(x)$ distributions will be the same and fall-off faster in x than the parent gluon distributions. In fact, measurements from Drell-Yan processes, deep inelastic electron and neutrino scattering, etc., show that these predictions are not correct.

The "five-quark" Fock state $|uudQ\bar{Q}\rangle$ is the most important origin of the sea-quark distributions of nucleon's The sea quarks determined by experiment have remarkable nonperturbative features, such as $\bar{u}(x) \neq \bar{d}(x)$, and an "intrinsic" strangeness [27] distribution at light-cone momentum fraction $x > 0.1$, as well as charm and bottom distributions at large x. In fact, recent measurements from HERMES show that the strange quark in the proton has two distinct components: a fast-falling contribution consistent with gluon splitting to $s\bar{s}$ and an approximately flat component up to $x < 0.5$. See fig. 1(a).

The proton's light-front wavefunction determined by the QCD LF Hamiltonian contains intrinsic heavy-quark Fock state multiply connected components such as $|uudc\bar{c}\rangle$. [8, 25, 28, 29] Such distributions [25, 28] favor configurations where the quarks have equal rapidity. The intrinsic heavy quarks thus carry most of the proton's momentum since t the off-shellness of the state is minimized. These configurations arise, for example, from $gg \to Q\bar{Q} \to gg$ insertions that are multiply-connected to the valence quarks in the hadronic self-energy diagram; See Fig. 1(b). in fact, the intrinsic strangeness, charm and $\bar{u}(x) - \bar{d}(x)$ distributions have a nearly universal form, [8] as recently shown by Chang and Peng. [30].

QCD also predicts that the color-configuration of the heavy quark pair $Q\bar{Q}$ in the intrinsic five-quark Fock state is primarily a color-octet; furthermore, the ratio of intrinsic charm to intrinsic bottom scales as $m_c^2/m_b^2 \simeq 1/10$, as can be shown using the operator product expansion in non-Abelian QCD. [25, 28] The intrinsic diagrams can thus explain the pen-charm and open-bottom hadron production at high momentum fractions, as can also account for single and double J/ψ hadroproduction measured by NA3 at high x_F.

In the case of a hadronic high energy proton collision, the high-x intrinsic charm quark in the proton's $|uudc\bar{c}>$ Fock state can coalesces with the co-moving ud valence quarks in a projectile proton to produce a $\Lambda_c(cud)$ baryon at the combined high momentum fraction $x_F = x_u + x_d + x_c$. Similarly, the coalescence of comoving b and $\bar{u}$ quarks from the $|uud\bar{b}b>$ intrinsic bottom Fock state explains the production of the $\Lambda_b(udb)$ which was first observed at the ISR collider at CERN by Cifarelli, Zichichi, and their collaborators [31]. Furthermore, one finds that the Λ_b is produced in association with a positron from the decay of the associated high-x_F $B^0(u\bar{b})$ meson.

As emphasized by Lai, Tung, and Pumplin [32], the structure functions used to model charm and bottom quarks in the proton at large x_{bj} have been consistently underestimated, since they ignore intrinsic heavy quark fluctuations of hadron wavefunctions. Furthermore, the neglect of the intrinsic-heavy quark component in the proton structure function can lead to an incorrect assessment of the gluon distribution at large x if it is assumed that sea quarks can only arise from gluon splitting [33]

The D0 collaboration [34] at the Tevatron has measured $\bar{p}p \to c + \gamma + X$ and $\bar{p}p \to b + \gamma + X$ at $p_T^\gamma \sim 120$ GeV/c. As seen in Fig. 1(c), the rate for $\bar{p}p \to b + \gamma X$ for bottom quark jets agrees well with NLO PQCD; in contrast, the charm jet plus photon cross section deviates strongly from the standard PQCD prediction for $p_T^\gamma > 60\ GeV/c$. This photon plus charm jet anomaly could well be explained if one allows for an intrinsic contribution to the charm structure function in $gc \to c\gamma$ at $Q^2 \sim 10^4$ GeV^2, but it requires a factor of two increase in strength compared to the CTEQ parameterization. This discrepancy could indicate that the reduction of the charm distribution due to DGLAP evolution has been overestimated.

Measurements by the SELEX collaboration [35] led to the discovery of a set of doubly-charmed spin 1/2 and spin 3/2 baryons with quantum numbers that can be identified as $|ccu\rangle$ and $|ccd\rangle$ bound states. The NA3 experiment has also observed the hadroproduction of two J/ψs at high x_F, also a signal for seven-quark Fock states like $|uudc\bar{c}c\bar{c}>$ in the proton. Surprisingly, the mass splittings of the ccu and ccd states measured by SELEX are much larger than

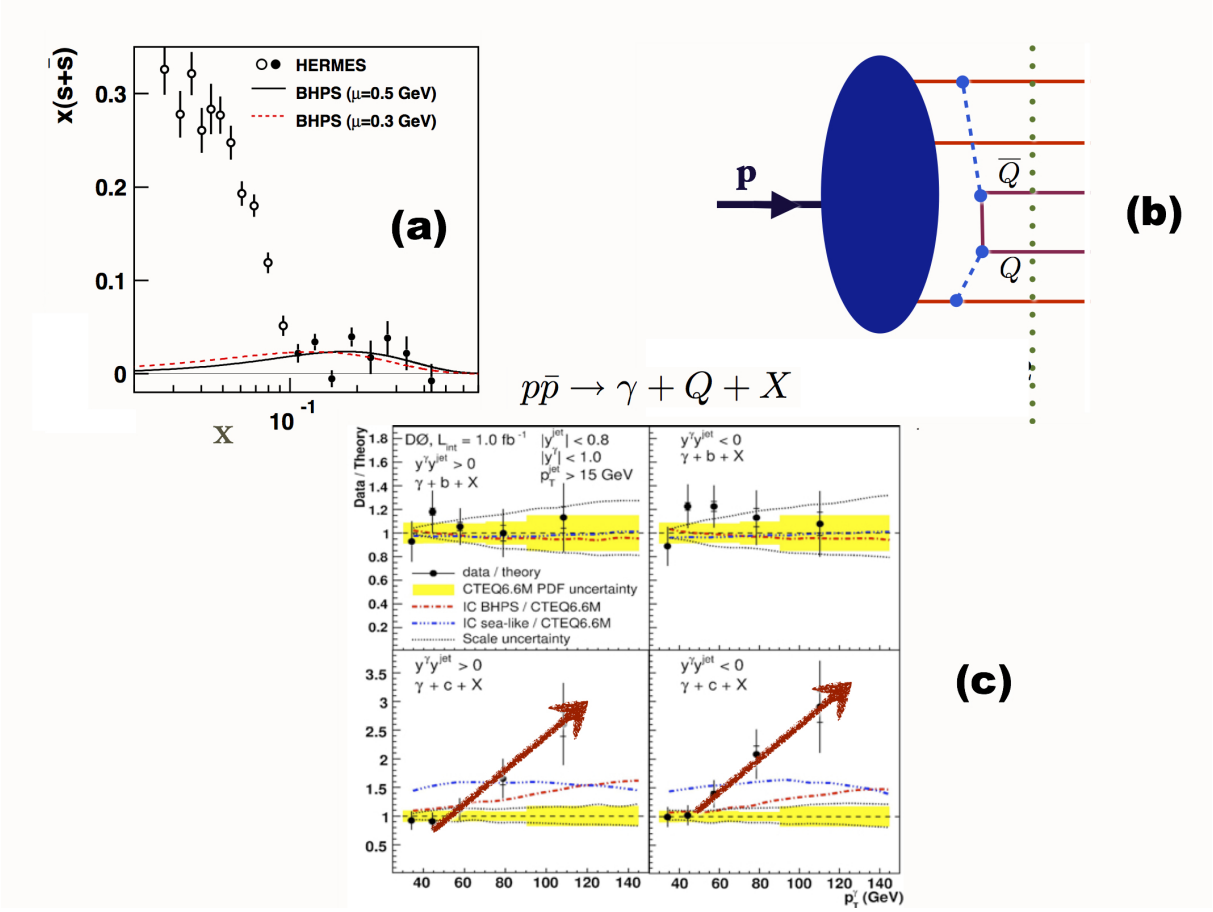

FIG. 1: (a) Intrinsic and extrinsic strangeness distribution. [30] (b) Five-quark Fock state of the proton and the origin of the intrinsic sea. (c) D0 measurement of $\bar{p}p \to \gamma + bX$ and $\bar{p}p \to \gamma + cX$.

expected from known QCD isospin-breaking effects.. One speculative proposal [36] is that these baryons have the configuration $c\ q\ c$ where the light quark q is exchanged between the heavy quarks as in a linear molecule. This configuration may enhance the Coulomb repulsion of the $c\ u\ c$ relative to $c\ d\ c$. It is clearly important to have experimental confirmation of the SELEX results.

The cross section for J/ψ production in a nuclear target is well measured. The ratio of the nuclear and proton target cross sections has the form $A^{\alpha(x_F)}$ where x_F is Feynman fractional longitudinal momentum of the J/ψ. At small x_F, $\alpha(x_F)$ is slightly smaller than one but at $x_F \sim 1$ it decreases to $\alpha = 2/3$. These results, as shown in Fig. 2(a), are surprising since (1) the value $\alpha = 2/3$ would be characteristic of a strongly interacting hadron, not a small-size quarkonium state; and (2) the functional dependence $A^{\alpha(x_F)}$ contradicts pQCD factorization predictions. This effect, in combination with the anomalously nearly flat cross sections at high x_F, points to a QCD mechanism based on color-octet intrinsic charm Fock states: large color dipole the intrinsic heavy quark Fock state of the proton: $|(uud)_{8_C}(c\bar{c})_{8_C}\rangle$ interacts primarily with the $A^{2/3}$nucleons at the front surface because of its large color-dipole moment. See Fig. 2(b). The $c\bar{c}$ color octet thus scatters on a front-surface nucleon, changes to a color singlet, and then propagates through the nucleus as a J/ψ at high x_F. Alternatively, one can postulate strong energy losses of a color octet $c\bar{c}$ state as it propagates in the nucleus but it is hard to see how this can account for the observed nearly flat behavior of the $A^{2/3}$ component as observed by NA3.

Multi-gluon processes such as $[gg] = g \to J/\psi$ can dominate quarkonium or even Higgs hadroproduction in the forward rapidity domain $y \sim 4$ at the LHC. The large interaction cross section $[gg]$ can lead to anomalously large shadowing.

Intrinsic heavy quarks leads to a novel mechanism for the inclusive and diffractive Higgs production $pp \to ppH$ where the Higgs boson carries a large fraction of the projectile proton momentum. [37, 38] This high x_F production mechanism is based on the subprocess $(Q\bar{Q})g \to H$ where the Higgs couples to the sum of the momentum of the $Q\bar{Q}$ pair in the $|uudQ\bar{Q}\rangle$ intrinsic heavy quark Fock state of the colliding proton; it thus can be produced with

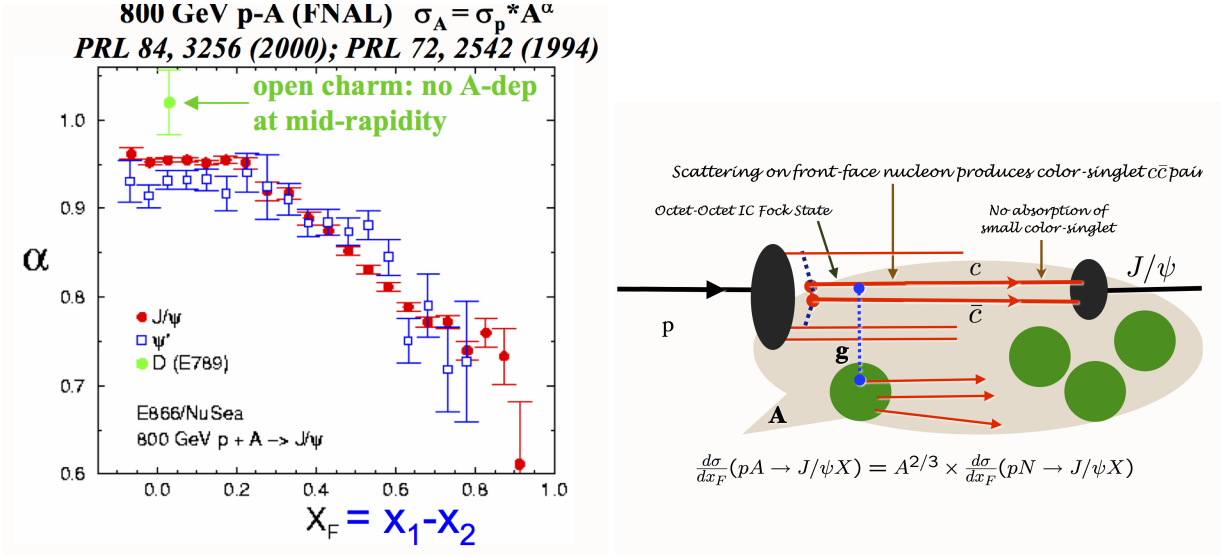

FIG. 2: (a) E866/NuSea data for the nuclear A dependence of J/ψ and ψ' hadroproduction. (b) Model for the A dependence of J/ψ hadroproduction based on color-octet intrinsic charm.

approximately 80% of the projectile proton's momentum. High-x_F Higgs production could be measured at the LHC using far forward detectors or arranging the proton beams to collide at a significant crossing angle. It is also possible to produce a light mass Higgs at threshold using the 7 TeV proton beam colliding with a fixed nuclear target.

IV. THE UNEXPECTED ROLE OF DIRECT PROCESSES IN HIGH p_T HADRON REACTIONS

It is conventional to assume that hadrons produced at high transverse momentum in inclusive high energy hadronic collisions such as $pp \to HX$ arise only from quark or gluon jet fragmentation. The simplest test of the leading-twist pQCD prediction in high transverse momentum hadronic reactions is to measure the power-law fall-off of the inclusive cross section [39] $Ed\sigma/d^3p(AB \to CX) = F(\theta_{cm}, x_T)/p_T^{n_{\rm eff}}$ at fixed $x_T = 2p_T/\sqrt{s}$ and fixed θ_{CM}. In the case of the scale-invariant parton model $n_{\rm eff} = 4$. However in QCD $n_{\rm eff} \sim 4 + \delta$ where $\delta \simeq 1.5$ is the QCD correction to conformal invariance due to the running of the QCD coupling and the DGLAP evolution of the input parton distribution and fragmentation functions. [40, 41]

One expects that the leading power-law contributions will dominate measurements of high p_T hadron production at RHIC and at Tevatron energies. Data for isolated photon production $pp \to \gamma_{\rm direct} X$, as well as jet production, in fact agree well with the leading-twist scaling prediction $n_{\rm eff} \simeq 4.5$. [40] In contrast, measurements of $n_{\rm eff}$ for hadron production are not consistent with the leading-twist predictions. See Fig. 3(a). Striking deviations from the leading-twist predictions have also been observed at lower energy at the ISR and Fermilab fixed-target experiments. [39] This can be explained if there are significant contributions from direct higher-twist processes – reactions where the hadron is created directly in the hard subprocess rather than from jet fragmentation.

QCD does predict that high $p_\perp^H$ isolated hadrons can be created from hard higher-twist subprocess [40, 41] at a significant rate, even at the LHC. [See, for example, Fig. 3(b).] This "direct" production of hadrons can also explain [42] the remarkable "baryon anomaly" observed at RHIC: the ratio of baryons to mesons at high $p_\perp^H$, as well as the power-law fall-off $1/p_\perp^n$ at fixed $x_\perp = 2p_\perp/\sqrt{s}$, both increase with centrality. [43] This is opposite to the expectation that protons should experience more energy loss than mesons in the nuclear medium. The high values $n_{\rm eff}$ with x_T seen in the data indicate the presence of an array of higher-twist processes, including subprocesses where the hadron enters directly, rather than through jet fragmentation. [44] Although they are suppressed by powers of $1/p_T$, the direct higher twist processes can dominate because they are energy efficient – no same side energy or momentum is lost from the undetected fragments. Thus the incident colliding partons are evaluated at the minimum possible values of light-front momentum fractions x_1 and x_2, where the parton distribution functions are numerically large.

Normally many more pions than protons are produced at high transverse momentum in hadron-hadron collisions. This is also true for the peripheral collisions of heavy ions. However, when the nuclei collide with maximal overlap (central collisions) the situation is reversed – more protons than pions emerge. This observation at RHIC [43]

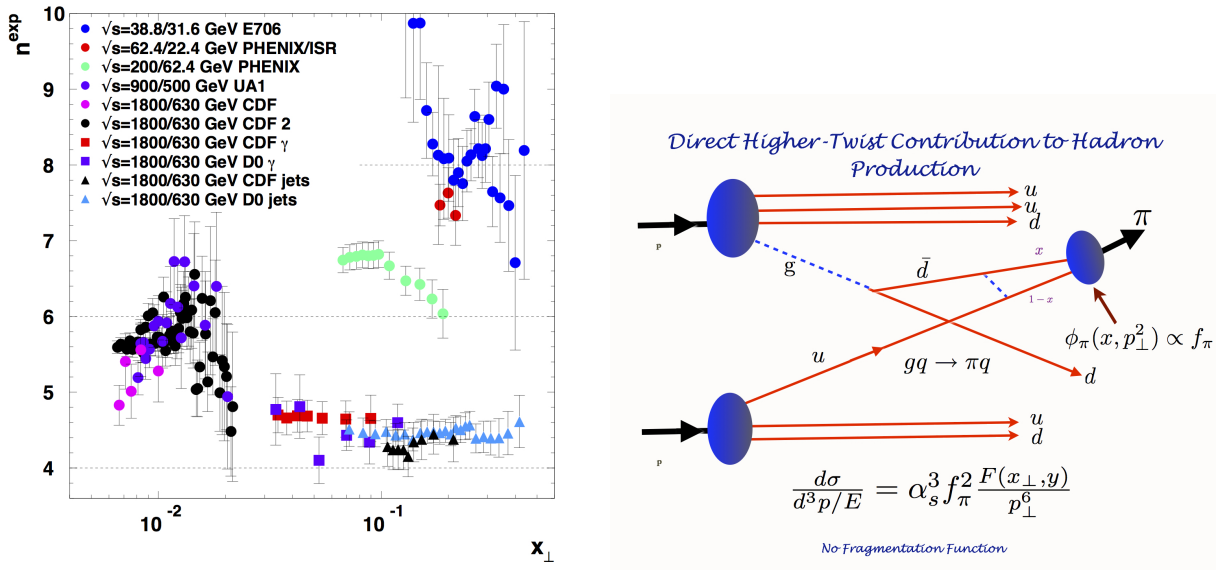

FIG. 3: (a) Scaling of inclusive cross sections for hadron, photons and jets at high p_T at fixed $x_T = 2\frac{p_T}{\sqrt{s}}$. (b) Example of a direct QCD contribution for pion production. [40, 41].

contradicts the usual expectation that protons should be more strongly absorbed than pions in the nuclear medium. This deviation also points to a significant contribution from direct higher twist processes where hadrons, particularly baryons are created directly in the hard subprocess rather than from quark or gluon jet fragmentation. Since these processes create color-transparent baryons, this mechanism can explain the RHIC baryon anomaly. [42]. Evidence for color transparency [23] is particularly clear in diffractive dijet production on nuclei [45]

V. BREAKDOWN OF PERTURBATIVE QCD FACTORIZATION THEOREMS

The factorization picture derived from the parton and pQCD has played a guiding role in virtually all aspects of hadron physics phenomenology. In the case of inclusive reactions such as $\frac{E_H d\sigma}{d^3 p_H}(pp \to HX)$, the pQCD ansatz predicts that the cross section at leading order in the transverse momentum p_T can be computed by convoluting the perturbatively calculable hard subprocess quark and gluon cross section with the process-independent structure functions of the colliding hadrons with the quark fragmentation functions. The resulting cross section scales as $1/p_T^4$, modulo the DGLAP scaling violations derived from the logarithmic evolution of the structure functions and fragmentation distributions, as well as the running of the QCD coupling appearing in the hard scattering subprocess matrix element.

The effects of final-state interactions of the scattered quark in deep inelastic scattering have been traditionally assumed to either give an inconsequential phase factor or power-law suppressed corrections. However, this is only true for sufficiently inclusive cross sections. For example, consider semi-inclusive deep inelastic lepton scattering (SIDIS) on a polarized target $\ell p_\uparrow \to H\ell' X$. In this case the final-state gluonic interactions of the scattered quark lead to a T-odd non-zero spin correlation of the plane of the lepton-quark scattering plane with the polarization of the target proton [15] which is not power-law suppressed with increasing virtuality of the photon Q^2; i.e. it Bjorken-scales. This leading-twist "Sivers effect" [14] is nonuniversal in the sense that pQCD predicts an opposite-sign correlation in Drell-Yan reactions relative to single-inclusive deep inelastic scattering. [16, 17] This important but yet untested prediction occurs because the Sivers effect in the Drell-Yan reaction is modified by the initial-state interactions of the annihilating antiquark.

Similarly, the final-state interactions of the produced quark with its comoving spectators in SIDIS produces a final-state T-odd polarization correlation – the "Collins effect". This can be measured without beam polarization by measuring the correlation of the polarization of a hadron such as the Λ baryon with the quark-jet production plane. Analogous spin effects occur in QED reactions due to the rescattering via final-state Coulomb interactions. Although the Coulomb phase for a given partial wave is infinite, the interference of Coulomb phases arising from different

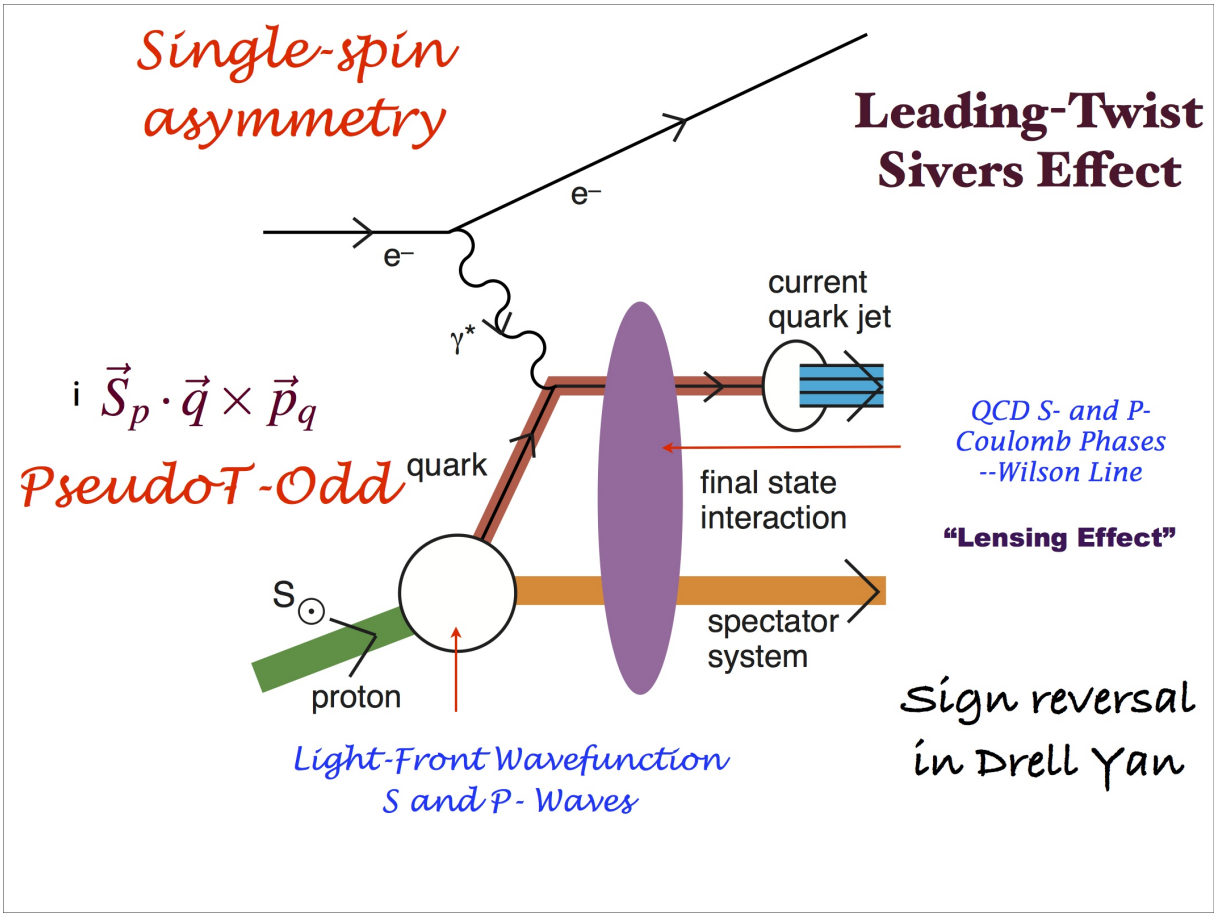

FIG. 4: Physics of the Sivers single-spin asymmetry in semi-inclusive deep inelastic lepton scattering.

partial waves leads to observable effects. These considerations have led to a reappraisal of the range of validity of the standard factorization ansatz. [46]

The calculation of the Sivers single-spin asymmetry in deep inelastic lepton scattering in QCD is illustrated in Fig. 4. The analysis requires two different orbital angular momentum components: S-wave with the quark-spin parallel to the proton spin and P-wave for the quark with anti-parallel spin; the difference between the final-state "Coulomb" phases leads to a $\vec{S}\cdot\vec{q}\times\vec{p}$ correlation of the proton's spin with the virtual photon-to-quark production plane. [15] Thus, as it is clear from its QED analog, the final-state gluonic interactions of the scattered quark lead to a T-odd non-zero spin correlation of the plane of the lepton-quark scattering plane with the polarization of the target proton. [15]

Both the S- and P-wave proton wavefunctions appear in the calculation of the Pauli form factor quark-by-quark. Thus one can correlate the Sivers asymmetry for each struck quark with the anomalous magnetic moment of the proton carried by that quark, [47]; this leads to the prediction that the Sivers effect is larger for positive pions. This has been observed by the HERMES, [48], COMPASS experiment [49–51] at CERN, and CLAS [52, 53]

QCD predicts an opposite-sign correlation [16, 17] in Drell-Yan reactions due to the initial-state interactions of the annihilating antiquark; the leading-twist Bjorken-scaling "Sivers effect" is thus nonuniversal. The $S-$ and P-wave proton wavefunctions also appear in the calculation of the Pauli form factor quark-by-quark. The physics of the "lensing dynamics" or Wilson-line physics [19] involves nonperturbative quark-quark interactions at small momentum transfer – not the hard scale Q^2. It may be possible to predict the strength of the soft initial- or final- state scattering using the effective confining potential derived from light-front holographic QCD.

Measurements [54] of the Drell-Yan Process $\pi p \to \mu^+\mu^- X$ show a nontrivial angular distribution contradicting pQCD expectations: one observes an anomalously large $\cos 2\phi$ azimuthal angular correlation between the lepton decay plane and its production plane, contradicting the Lam-Tung relation, a prediction of pQCD factorization. [55] Such effects again point to the importance of initial and final-state interactions of the hard-scattering constituents, [56] corrections not included in the standard pQCD factorization formalism.

Collins and Qiu [46] have shown that the traditional factorization formalism of perturbative QCD fails for angular

correlations in general hard inclusive reactions because of the lensing effects of initial and final-state interactions. For example, if both the quark and antiquark in the Drell-Yan subprocess $q\bar{q} \to \mu^+\mu^-$ interact with the spectators of the other incident hadron projectile, then one predicts a $\cos 2\phi \sin^2\theta$ planar correlation in unpolarized Drell-Yan reactions. [56] This "double" Boer-Mulders effect can explain the large $\cos 2\phi$ correlation and the corresponding violation [56, 57] of the Lam Tung relation for Drell-Yan processes which was observed by the NA10 collaboration. [54] In each case one see the importance of initial and final-state interactions of the hard-scattering constituents, in contrast to standard pQCD factorization.. Large single spin asymmetries in reactions such as $pp_\uparrow \pi X$, an effect not yet explained in the usual formulation of pQCD. [58]. It may indicate subprocesses involving multiparton from the initial hadron. A possible signal for factorization breakdown at the LHC will be the observation of a $\cos 2\phi$ planar correlation in dijet production.

The final-state rescattering of the struck quark with the target spectators [20] leads to diffractive events in deep inelastic scattering (DDIS) at leading twist, where the proton remains intact and isolated in rapidity such as $\ell p \to \ell' p' X$; in fact, 10 % to 15% of the deep inelastic lepton-proton scattering events observed at HERA are diffractive. [59, 60] although the underlying hard subprocess $\ell q \to \ell' q'$ is highly disruptive of the target nucleon.

The presence of a rapidity gap between the target and diffractive system – keeping the target remnant in its color-singlet state – is made possible in any gauge by the soft rescattering incorporated in the Wilson line or the light-front wavefunctions. Different fractions of single $pp \to \mathrm{Jet}\, p' X$ and double diffractive $p\bar{p} \to \mathrm{Jet}\, p'\bar{p}' X$ events are observed at the Tevatron. This is expected from soft gluon exchange between the scattered quark and the remnant system occurring after the hard scattering.

Stodolsky [61] has shown, using Gribov-Glauber theory, that the leading twist diffractive deep inelastic scattering events lead to the shadowing of nuclear structure functions at small $x_{\rm Bjorken}$, due to the destructive interference of two-step and one step amplitudes in the nucleus. Since diffraction involves rescattering, shadowing and diffractive processes are not intrinsic properties of hadron and nuclear wavefunctions and structure functions; they are, instead, properties of the complete dynamics of the scattering reaction. [62]

VI. FLAVOR-DEPENDENT ANTISHADOWING

The nuclear modifications to the structure functions measured in deep inelastic charged lepton-nucleus and neutrino-nucleus interactions are usually assumed to be identical. In fact, t Gribov-Glauber theory predicts that antishadowing of nuclear structure functions is not universal, but instead depends on the quantum numbers of each struck quark and antiquark. [22] A recent analysis by Schienbein *et al.* [63] in fact shows that the NuTeV measurements of nuclear structure functions obtained from neutrino charged current reactions differ significantly from the distributions measured in deep inelastic electron and muon scattering. See Fig. 5.

Empirically, one finds $R_A(x,Q^2) \equiv$
$\big(F_{2A}(x,Q^2)/(A/2)F_d(x,Q^2)\big) > 1$ in the domain $0.1 < x < 0.2$; i.e., the measured nuclear structure function (referenced to the deuteron) is larger than the scattering on A nucleons. Leading-twist diffractive contributions $\gamma^* N_1 \to (q\bar{q})N_1$ can arise from Reggeon exchange in the t-channel.; e.g., isospin–non-singlet $C = +$ Reggeons. This contributes to the difference of proton and neutron structure functions, giving the characteristic Kuti-Weiskopf Regge $F_{2p} - F_{2n} \sim x^{1-\alpha_R(0)} \sim x^{0.5}$ behavior at small x. This dependence of the structure functions reflects the Regge behavior $\nu^{\alpha_R(0)}$ of the forward virtual Compton amplitude. $t = 0$. The phase of the diffractive amplitude, which is determined by analyticity and crossing, is proportional to $-1 + i$ for $\alpha_R = 0.5$, which together with the phase from the Glauber cut, leads to the *constructive* interference of the diffractive and nondiffractive multi-step nuclear amplitudes. The nuclear structure function is thus enhanced [64] in the domain $0.1 < x < 0.2$ where antishadowing is observed. The strength of the Reggeon amplitudes is fixed by Regge behavior of the nucleon structure functions, so there is little model dependence. Since quarks of different flavors couple to different Reggeons, nuclear antishadowing is flavor-dependent and thus not universal; [22]. This picture allows substantially different antishadowing for charged and neutral current reactions, thus affecting the analysis of the weak-mixing angle θ_W. The anomalous result for θ_W reported by NuTeV may be related to the non-universality of nuclear antishadowing.

VII. DYNAMIC VERSUS STATIC HADRONIC STRUCTURE FUNCTIONS

The effects of rescattering and diffraction highlight the need for a fundamental understanding the dynamics of hadrons in QCD at the amplitude level. This is important for understanding the quantum mechanics of hadron formation, the lensing effects of initial and final interactions, the origin of diffractive phenomena and single-spin asymmetries, as well as higher-twist semi-exclusive hadron subprocesses.

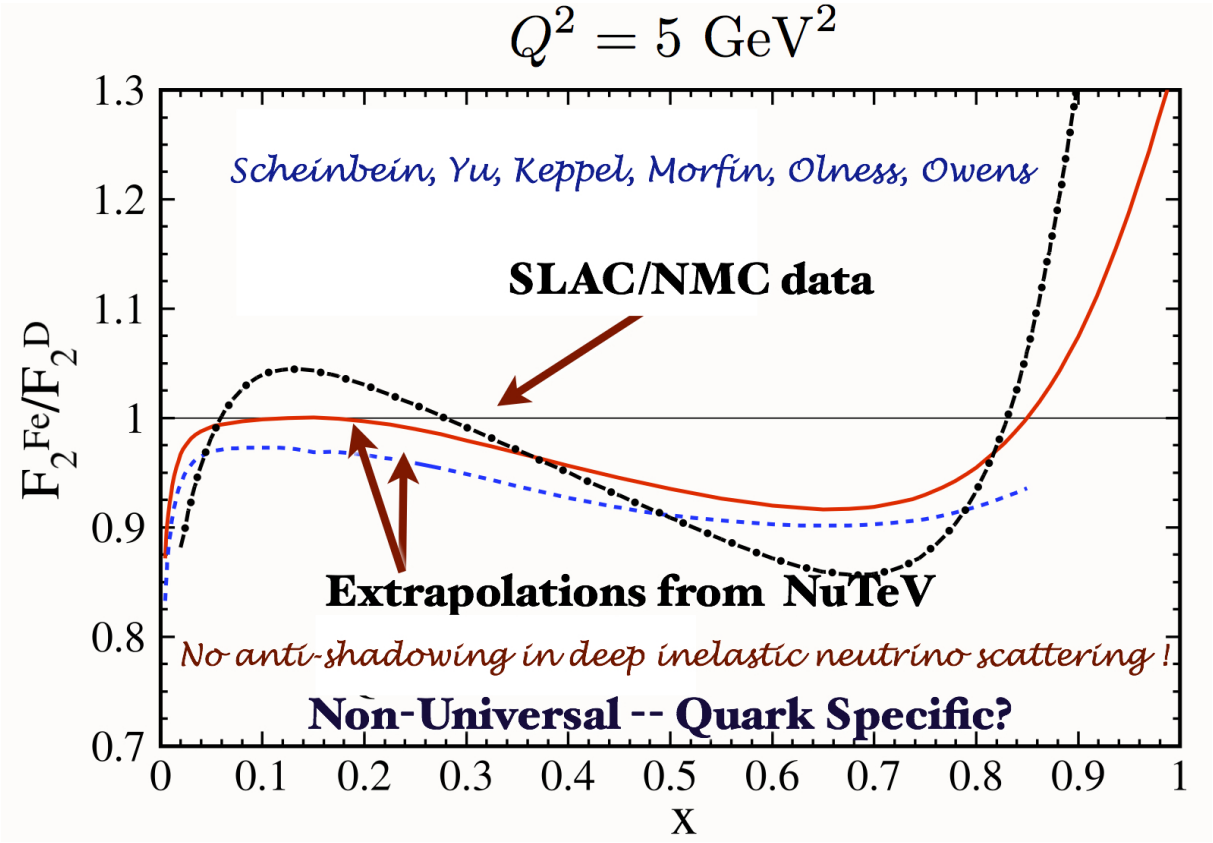

FIG. 5: Evidence for nonuniversal antishadowing.

In the parton model the structure functions measured in deep inelastic scattering can be computed at leading-twist limit from the absolute square of the light-front wavefunctions, summed over all Fock states. However, as I have discussed, dynamical effects, such as the Sivers spin correlation and diffractive deep inelastic lepton scattering due to final-state gluon interactions, contribute to the observed deep inelastic lepton-hadron cross sections. Diffractive events lead to the interference of two-step and one-step processes in nuclei which in turn, via the Gribov-Glauber theory, lead to the shadowing and the antishadowing of the deep inelastic nuclear structure functions; [22]. The real wavefunctions of hadrons cannot describe diffractive deep inelastic scattering nor single-spin asymmetries, since such phenomena involve the complex phase structure of the $\gamma^* p$ amplitude. Since lensing phenomena are not included in the light-front wavefunctions of the nuclear eigenstate, one should distinguished between "dynamical" vs. "static" (wavefunction-specific) structure functions. [21] See Fig. 6. It is possible to augment the light-front wavefunctions with a gauge link corresponding to an external field created by the virtual photon $q\bar{q}$ pair current, [65, 66] but such a gauge link is process dependent. [16] Thus the physics of rescattering and nuclear shadowing is not included in the nuclear light-front wavefunctions and a probabilistic interpretation of the nuclear DIS cross section in terms of hadron structure is thus precluded in principle, although it can often be treated as an effective approximation.

VIII. THE PRINCIPLE OF MAXIMUM CONFORMALITY AND THE ELIMINATION OF THE RENORMALIZATION SCALE AMBIGUITY

A key difficulty in making precise perturbative QCD predictions is the uncertainty in determining the renormalization scale μ of the running coupling $\alpha_s(\mu^2)$. It is common practice to simply guess a physical scale $\mu = Q$ of order of the momentum transfer Q in the process; one then varies the guessed scale over a range $Q/2$ and $2Q$. This procedure is clearly problematic, since the resulting fixed-order pQCD prediction will depend on the choice of renormalization scheme; it can even predict negative QCD cross sections at next-to-leading-order.

If one chooses the renormalization scale to have minimum sensitivity, one typically obtains an incorrect answer in QED. The prediction violates the transitivity property of the renormalization group and depends on the choice

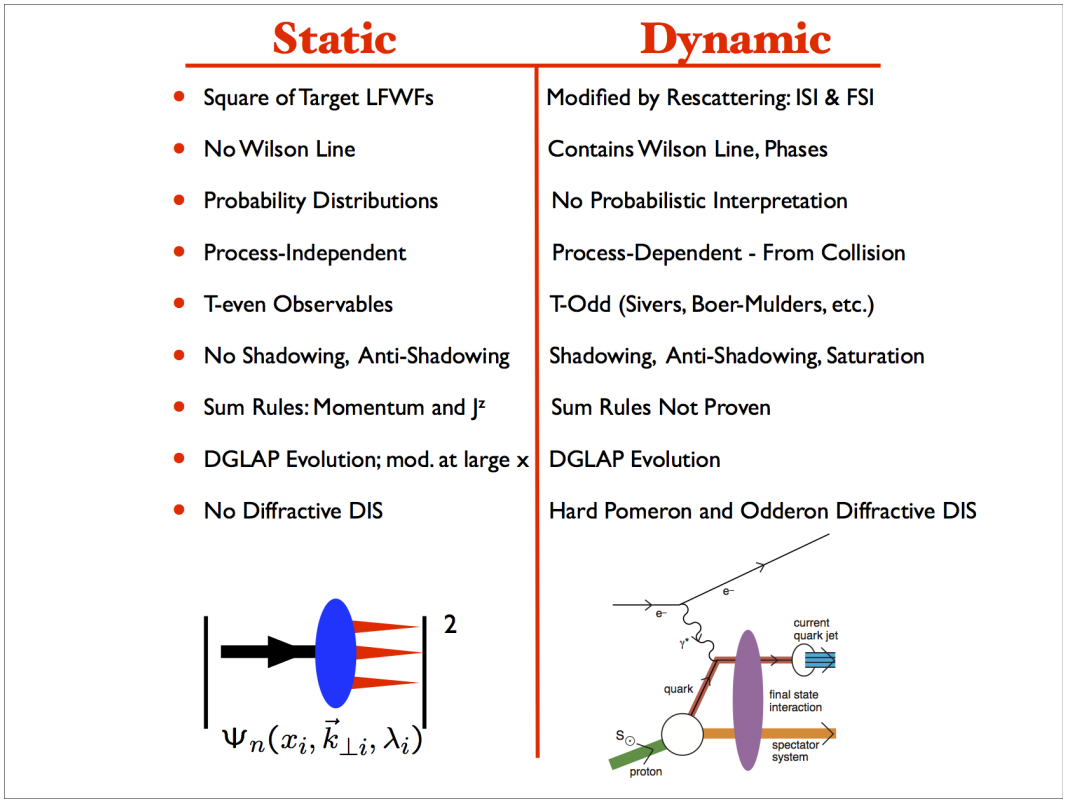

FIG. 6: Static versus dynamic structure functions.

of renormalization scheme. in the case of $e^+e^- \to q\bar{q}g$ (three-jet events). [67], the predicted renormalization scale incorrectly vanishes as the gluon jet virtuality increases [67].

The running coupling in a gauge theory sums the terms involving the β function; thus when the renormalization scale is set properly, all non-conformal $\beta \neq 0$ terms in a perturbative expansion arising from renormalization are summed into the running coupling. The remaining terms in the perturbative series will then be identical to those of a conformal theory; i.e., the corresponding theory with $\beta = 0$. As discussed by Di Giustino, Wu, Mojaza, and myself [68–70], the resulting scale-fixed predictions using this "principle of maximum conformality" (PMC) are independent of the choice of renormalization scheme – as required physically and by by the renormalization group. The PMC is the principle [68, 69] which underlies the BLM scale-setting method. [71] The PMC/BLM scales are fixed order-by-order. The BLM/PMC scale then automatically determines the number of effective flavors in the β-function. The results avoid the divergent renormalon resummation and agree with QED scale-setting in the Abelian limit. In the case of QED, the PMC scale is proportional to the photon virtuality and thus sums all vacuum polarization corrections to all orders. Different schemes lead to different effective PMC/BLM scales, but the final results are scheme independent. One also obtains scheme-independent commensurate scale relations connecting different observables, and determines the scale displacements among the PMC/BLM scales which are derived under different schemes. The PMC procedure is also valid for multi-scale processes.

One can also introduce a generalization of conventional dimensional regularization, the $\mathcal{R}_\delta$ schemes. For example, when one generalizes the MSBar scheme by subtracting $\ln 4\pi - \gamma_E - \delta$ instead of just $\ln 4\pi - \gamma_E$ the new terms generated in the pQCD series proportional to δ expose the β terms and thus the renormalization scheme dependence. Thus the $\mathcal{R}_\delta$ schemes uncover the renormalization scheme and scale ambiguities of pQCD predictions, exposes the general pattern of nonconformal terms, and allows one to systematically determine the argument of the running coupling order by order in pQCD in a form which can be readily automatized [70, 72]. The resulting PMC scales and finite-order PMC predictions are to high accuracy independent of the choice of initial renormalization scale. For example, PMC scale-setting leads to a scheme-independent pQCD prediction [73] for the top-quark forward-backward asymmetry which is within one σ of the Tevatron measurements. The PMC satisfies all of the principles of the renormalization group: reflectivity, symmetry, and transitivity, and it thus eliminates an unnecessary source of systematic error in pQCD predictions [76]. The BLM/PMC also provides scale-fixed, scheme-independent high-precision connections between observables, such

as the "Generalized Crewther Relation", [75] as well as other "Commensurate Scale Relations". [74, 77] .

Thus by using the PMC/BLM procedure [71], all non-conformal contributions in the perturbative expansion series are incorporated into the running coupling by shifting the renormalization scale in α_s from its initial value, and one obtains unique, scale-fixed, scheme-independent predictions at any finite order. The BLM/PMC method gives results which are independent of the choice of renormalization scheme at each order of perturbation theory, as required by the transitivity property of the renormalization group. The argument of the running coupling constant acquires the appropriate displacement appropriate to its scheme, so that the evaluated result is scheme-independent. The elimination of the renormalization scheme ambiguity improves the accuracy of pQCD tests and increases the sensitivity of LHC experiments and other measurements to new physics beyond the Standard Model.

IX. ADS/QCD AND LIGHT-FRONT HOLOGRAPHY

An important goal in hadron physics is to find an analytic first approximation to QCD which is relativistic, frame-independent color-confining, and consistent with chiral symmetry. de Téramond and I [4] have shown that the gauge/gravity duality leads to a simple analytical and phenomenologically compelling nonperturbative approximation to the full light-front QCD Hamiltonian – "Light-Front Holography". [4] Light-Front Holography is a remarkable feature of the AdS/CFT correspondence. [78] One finds that the "soft-wall" AdS/QCD model, modified by a positive-sign dilaton metric, leads to a simple Schrödinger-like light-front wave equation and a one-parameter description of nonperturbative hadron dynamics [4, 79]. The model predicts a zero-mass pion for massless quarks and a Regge spectrum of linear trajectories with the same slope in the (leading) orbital angular momentum L of the hadrons and their radial quantum number n.

Light front holographic methods connect the functional dependence of the wavefunction $\Phi(z)$ computed in the AdS fifth dimension to the hadronic frame-independent light-front wavefunction $\psi(x_i, b_{\perp i})$ in $3+1$ physical space-time. The variable z maps to a transverse LF variable $\zeta(x_i, b_{\perp i})$ which is conjugate to the off-shell invariant mass of the constituents. The result is a single-variable light-front Schrödinger equation which determines the eigenspectrum and the LFWFs of hadrons for general spin and orbital angular momentum. The transverse coordinate ζ is closely related to the invariant mass squared of the constituents in the LFWF and its off-shellness in the LF kinetic energy, and it is thus the natural variable to characterize the hadronic wavefunction. In fact ζ is the only variable to appear in the relativistic light-front Schrödinger equations predicted from holographic QCD in the limit of zero quark masses. The coordinate z in AdS space is thus uniquely identified with a Lorentz-invariant coordinate ζ which measures the separation of the constituents within a hadron at equal light-front time. This duality provides a semi-classical frame-independent first approximation to the spectra and light-front wavefunctions of meson and baryon light-quark bound states. One also predicts hadron dynamics, such as the behavior of the pion and nucleon form factors.

The resulting hadron eigenstates can have valence components with different orbital angular momentum; e.g., the proton eigenstate in AdS/QCD with massless quarks has $L^z = 0$ and $L^z = 1$ light-front Fock components with equal probability. Thus in this approach, the spin of the proton is carried by quark orbital angular momentum: $J^z = \langle L^z \rangle = \pm 1/2$ since $\langle \sum S^z_q \rangle = 0$, [80] helping to explain the "spin-crisis".

The AdS/QCD soft-wall model also predicts the form of the non-perturbative effective coupling $\alpha_s^{AdS}(Q)$ as shown in fig. 7(d) and its β-function in excellent agreement with JLAB measurements. [81] The AdS/QCD light-front wavefunctions also lead to a proposal for computing the hadronization of quark and gluon jets at the amplitude level. [26]

In general the QCD Light-Front Hamiltonian can be systematically reduced to an effective equation in acting on the valence Fock state. This is illustrated for mesons in fig. 7 The kinetic energy contains a term L^2/ζ^2 analogous to $\ell(\ell+1)/r^2$ in nonrelativistic theory, where the invariant $\zeta^2 = x(1-x)b_\perp^2$ is conjugate to the $q\bar{q}$ invariant mass $k_\perp^2/x(1-x)$. The variable ζ plays the role of the radial variable r. Here $L = L^z$ is the projection of the orbital angular momentum appearing in the ζ, ϕ basis. The AdS/QCD model has the identical structure as the reduced form of the LF Hamiltonian, but it also specifies the confining potential as $U(\zeta, S, L) = \kappa^4 \zeta^2 + \kappa^2(L + S - 1/2)$. The observation that AdS/QCD formulae for elastic electromagnetic and gravitational form factors match the LF Drell-Yan West formula, is the basis for light-front holography.

Light-quark meson and baryon spectroscopy is well described if one takes the only mass parameter $\kappa \simeq 0.55$ GeV. The linear trajectories in $M_H^2(n, L)$ have the same slope in L and n, the radial quantum number. AdS/QCD, together with Light-Front Holography [4] thus provides a simple Lorentz-invariant color-confining approximation to QCD which is successful in accounting for light-quark meson and baryon spectroscopy as well as their LFWFs. This semiclassical approximation to light-front QCD will break down at short distances where hard gluon exchange and other quantum corrections become important. The model can be systematically improved by Lippmann-Schwinger methods [82] or by using the AdS/QCD orthonormal basis to diagonalize the LF Hamiltonian. One can extend the semiclassical approximation by introducing nonzero quark masses and short-range Coulomb corrections, thus allowing predictions

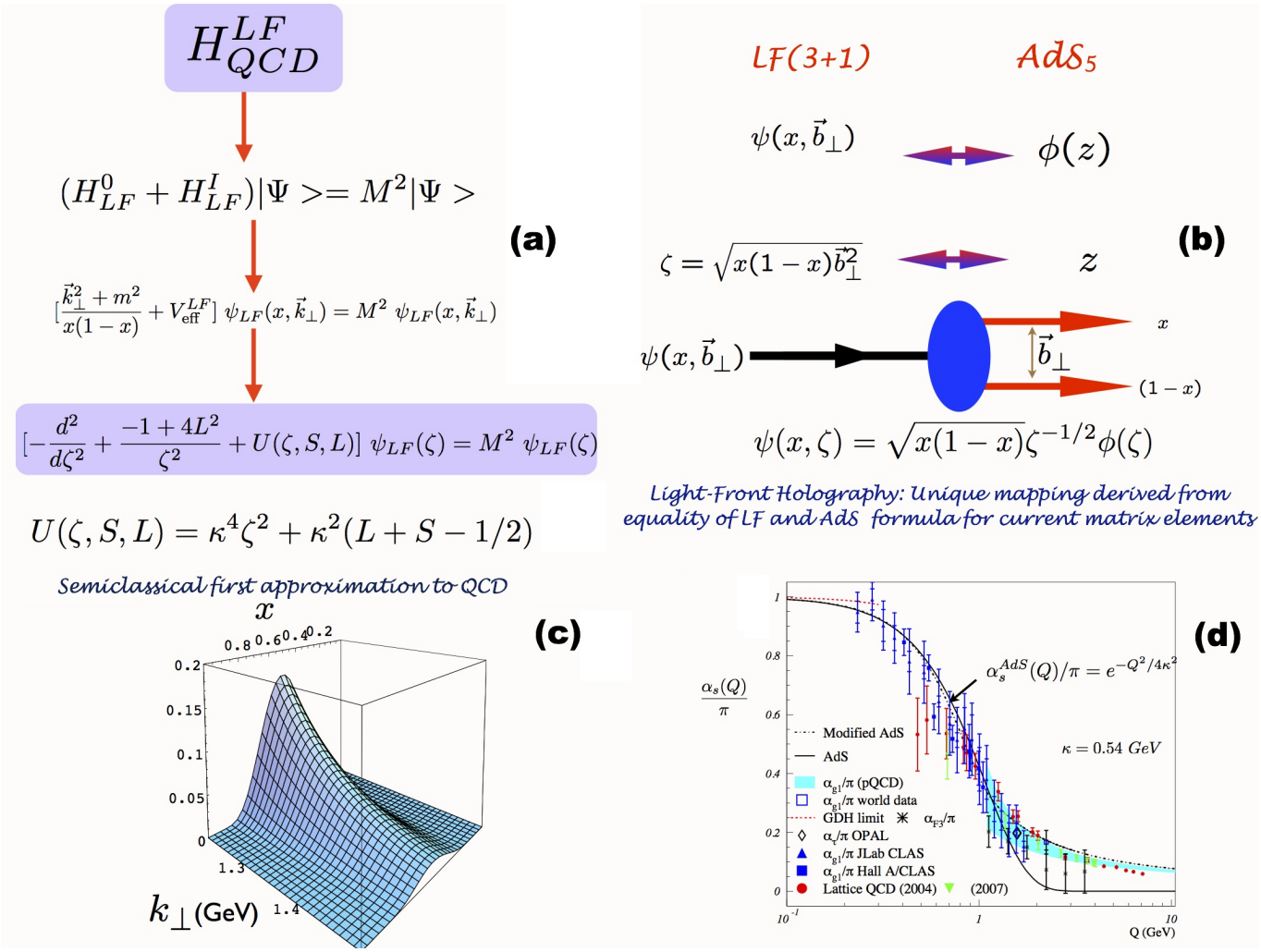

FIG. 7: (a) Reduction of the Light-Front Hamiltonian to an effective LF Schrodinger Equation for mesons. (b) Mapping of the fifth dimension coordinate z to the invariant LF separation variable ζ. The insert (c) shows the AdS/QCD – light-front holography prediction for the pion's valence LFWF $\psi(x, \mathbf{k}_\perp)$. (d) The running coupling predicted by AdS/QCD normalized to $\alpha_s/\pi = 1$ compared with the effective charge defined from the Bjorken sum rule. From Ref. [4].

for the dynamics and spectra of heavy and heavy-light quark systems. [83]

X. UNIQUENESS OF THE CONFINING POTENTIAL

If one starts with a dilaton profile $e^{\varphi(z)}$ with $\varphi \propto z^s$, the existence of a massless pion in the limit of massless quarks determines uniquely the value $s = 2$. To show this, one can use the stationarity of bound-state energies with respect to variation of parameters. More generally, the effective theory should incorporate the fundamental conformal symmetry of the four-dimensional classical QCD Lagrangian in the limit of massless quarks. To this end, deT'eramond, Dosch, and I [84] have studied the invariance properties of a one-dimensional field theory under the full conformal group following the dAFF construction of Hamiltonian operators described in Ref. [85].

One starts with the one-dimensional action

$$\mathcal{S} = \frac{1}{2}\int dt \left(\dot{Q}^2 - \frac{g}{Q^2}\right), \tag{1}$$

which is invariant under conformal transformations in the variable t. In addition to the Hamiltonian $H_t(Q,\dot{Q}) = \frac{1}{2}\left(\dot{Q}^2 + \frac{g}{Q^2}\right)$ there are two more invariants of motion for this field theory, namely the dilation operator D and K,

corresponding to the special conformal transformations in t. Specifically, if one introduces the the new variable τ defined through $d\tau = dt/(u + v\,t + w\,t^2)$ and the rescaled fields $q(\tau) = Q(t)/(u + v\,t + w\,t^2)^{1/2}$, it then follows that the the operator $G = u\,H_t + v\,D + w\,K$ generates the quantum mechanical evolution in τ [85]. The Hamiltonian corresponding to the operator G, which introduces the mass scale, is a linear combination of the old Hamiltonian H_t, D, the generator of dilations, and K, the generator of special conformal transformations. One can show explicitly [84, 85] that a confinement length scale appears in the action when one expresses the action in terms of the new time variable τ and the new fields $q(t)$, without affecting its conformal invariance. Furthermore, for $g \geq -1/4$ and $4\,uw - v^2 > 0$ the corresponding Hamiltonian $H_\tau(q,\dot{q}) = \frac{1}{2}\Big(\dot{q}^2 + \frac{g}{q^2} + \frac{4\,uw - v^2}{4} q^2\Big)$ is a compact operator. Finally, we can transform back to the original field operator $Q(t)$. We find

$$\begin{aligned} H_\tau(Q,\dot{Q}) &= \frac{1}{2}u\Big(\dot{Q}^2 + \frac{g}{Q^2}\Big) - \frac{1}{4}v\Big(Q\dot{Q} + \dot{Q}Q\Big) + \frac{1}{2}wQ^2 \\ &= uH_t + vD + wK, \end{aligned} \tag{2}$$

at $t = 0$. We thus recover the evolution operator $G = uH_t + vD + wK$ which describes the evolution in the variable τ, but expressed in terms of the original field Q.

The Shrödinger picture follows by identifying $Q \to x$ and $\dot{Q} \to -i\frac{d}{dx}$. Then the evolution operator in the new time variable τ is

$$H_\tau = \frac{1}{2}u\Big(-\frac{d^2}{dx^2} + \frac{g}{x^2}\Big) + \frac{i}{4}v\Big(x\frac{d}{dx} + \frac{d}{dx}x\Big) + \frac{1}{2}wx^2 \tag{3}$$

If we now compare the Hamiltonian (3) with the light-front wave equation and identify the variable x with the light-front invariant variable ζ, we have to choose $u = 2$, $v = 0$ and relate the dimensionless constant g to the LF orbital angular momentum, $g = L^2 - 1/4$, in order to reproduce the light-front kinematics. Furthermore $w = 2\lambda^2$ fixes the confining light-front potential to a quadratic $\lambda^2\,\zeta^2$ dependence. The mass scale brought in via $w = 2\kappa^2$ then generates the confining mass scale κ. The dilaton is also unique: $e^{\phi(z)} = e^{\kappa^2 z^2}$, where z^2 is matched to $\zeta^2 = b_\perp^2\,x(1-x)$ via LF holography. The spin-J representations in AdS_5 [86] then leads uniquely to the LF confining potential $U(\zeta^2) = \kappa^4\zeta^2 - 2\kappa^2(J-1)$.

The new time variable τ is related to the variable t for the case $uw > 0$, $v = 0$ by

$$\tau = \frac{1}{\sqrt{u\,w}} \arctan\left(\sqrt{\frac{w}{u}}t\right), \tag{4}$$

i.e., τ has only a limited range. The finite range of invariant LF time $\tau = x^+/P^+$ can be interpreted as a feature of the internal frame-independent LF time difference between the confined constituents in a bound state. For example, in the collision of two mesons, it would allow one to compute the LF time difference between the two possible quark-quark collisions [84].

XI. QCD CONDENSATES AND THE COSMOLOGICAL CONSTANT

It is often argued that the vacuum of QCD contains quark $\langle 0|q\bar{q}|0\rangle$ and gluon $\langle 0|G^{\mu\nu}G_{\mu\nu}|0\rangle$ vacuum condensates. These condensates are considered to be properties of the QCD vacuum and thus are assumed to be constant throughout space-time. However [87], this vacuum energy density leads to a 10^{45} order-of-magnitude discrepancy with the measured cosmological constant. This conflict is called "one of the gravest puzzles of theoretical physics;" and has been used as an argument for the anthropic principle. [88] A resolution of this long-standing puzzle has been suggested [89], motivated by Bethe-Salpeter and light-front analyses in which the QCD condensates are identified as "in-hadron" condensates, rather than vacuum entities [90]. The "in-hadron" condensates become realized as higher Fock states of the hadron when the theory is quantized at fixed light-front time $\tau = t - z/c$.

Recently a new perspective on the nature of QCD condensates $\langle\bar{q}q\rangle$ and $\langle G_{\mu\nu}G^{\mu\nu}\rangle$ has been presented. [89, 91, 94] A key ingredient in this approach is the use of Dirac's "Front Form"; [92]. In this formulation the spatial support of condensates is restricted to the interior of hadrons, since in the LF vacuum is an empty Fock state. Thus condensates arise due to the interactions of quarks and gluons which are confined within hadrons.

It is important to distinguish two very different concepts of the vacuum in quantum field theories such as QED and QCD. The instant-form vacuum is a state defined at the same time t at all spatial points in the universe. In contrast, the front-form vacuum only senses phenomena which are causally connected; i.e., within the observer's light-cone. The instant-form vacuum is defined as the lowest energy eigenstate of the instant-form Hamiltonian. For example, the instant-form vacuum in QED is saturated with quantum loops of leptons and photons. In calculations

of physical processes one must then normal-order the vacuum and divide the S-matrix elements by the disconnected vacuum loops. In contrast, the front-form (light-front) vacuum is defined as the lowest mass eigenstate of light-front Hamiltonian defined by quantizing at fixed $\tau = t - z/c$. The vacuum is remarkably simple in light-front quantization because of the restriction $k^+ \geq 0$. For example QED vacuum graphs such as $e^+e^-\gamma$ do not arise. The LF vacuum thus coincides with the vacuum of the free LF Hamiltonian. The front-form vacuum and its eigenstates are causal and Lorentz invariant; whereas the instant form vacuum depends on the observer's Lorentz frame. The instant-form vacuum is a state defined at the same time t at all spatial points in the universe. In contrast, the front-from vacuum only senses phenomena which are causally connected; i.e., or within the observer's light-cone. Causality in quantum field theory follows the fact that commutators vanish outside the light-cone. In fact in the LF analysis the spatial support of QCD condensates is restricted to the interior of hadrons, physics which arises due to the interactions of confined quarks and gluons. In the Higgs theory, the usual Higgs vacuum expectation value is replaced with a $k^+ = 0$ zero mode; [93] however, the resulting phenomenology is identical to the standard analysis.

When one makes a measurement in hadron physics, such as deep inelastic lepton-proton scattering, one probes hadron's constituents consistent with causality – at a given light front time, not at instant time. Similarly, when one makes observations in cosmology, information is obtained within the causal horizon; i.e., consistent with the finite speed of light. The cosmological constant measures the matrix element of the energy momentum tensor $T^{\mu\nu}$ in the background universe. It corresponds to the measurement of the gravitational interactions of a probe of finite mass; it only senses the causally connected domain within the light-cone of the observer. If the universe is empty, the appropriate vacuum state is thus the LF vacuum since it is causal. One automatically obtains a vanishing cosmological constant from the LF vacuum. Thus, as argued in Refs. [89, 91, 94] , the 45 orders of magnitude conflict of QCD with the observed value of the cosmological condensate is removed, and a new perspective on the nature of quark and gluon condensates in QCD is thus obtained.

In fact, in the LF analysis one finds that the spatial support of QCD condensates is restricted to the interior of hadrons, physics which arises due to the interactions of color-confined quarks and gluons. The condensate physics normally associated with the instant-form vacuum is replaced by the dynamics of higher non-valence Fock states as shown in the context of the infinite momentum/light-front method by Casher and Susskind. [95] and Burkardt [96] In particular, chiral symmetry is broken in a limited domain of size $1/m_\pi$, in analogy to the limited physical extent of superconductor phases. This novel description of chiral symmetry breaking in terms of "in-hadron condensates" has also been observed in Bethe-Salpeter studies. [97–101] The usual argument for a quark vacuum condensate is the Gell-Mann–Oakes–Renner (GMOR) formula: $m_\pi^2 = -2m_q\langle 0|\bar{q}q|0\rangle/f_\pi^2$. However, in the Bethe-Salpeter and light-front formalisms, where the pion is a $q\bar{q}$ bound-state, the GMOR relation is replaced by $m_\pi^2 = -2m_q\langle 0|\bar{q}\gamma_5 q|\pi\rangle/f_\pi$, where $\rho_\pi \equiv -\langle 0|\bar{q}\gamma_5 q|\pi\rangle$ represents a pion decay constant via an an elementary pseudoscalar current. The result is independent of the renormalization scale. In the light-front formalism, this matrix element derives from the $|q\bar{q}\rangle$ Fock state of the pion with parallel spin-projections $S^z = \pm 1$ and $L^z = \mp 1$, which couples by quark spin-flip to the usual $|q\bar{q}\rangle$ $S^z = 0, L^z = 0$ Fock state via the running quark mass. Thus again one finds "in-hadron condensates" replacing vacuum condensates: the $\langle 0|\bar{q}\bar{q}|0\rangle$ vacuum condensate which appears in the Gell-Mann Oakes Renner formula is replaced by the $\langle 0|\bar{q}\gamma_5|\pi\rangle$ pion decay constant. This new perspective also explains the results of studies [102–104] which find no significant signal for the vacuum gluon condensate.

XII. CONCLUSIONS

I have discussed a number of areas where conventional wisdom in hadron physics has been challenged:

1. The heavy quark sea is usually assumed to arise solely from the $g \to Q\bar{Q}$ subprocess, and it is thus confined to the low x domain; however, intrinsic contributions [8] arise from subprocesses where the heavy quarks are multi-connected to the valence quarks. The intrinsic $Q\bar{Q}$ contributions appear dominantly at the same rapidity as the valence quarks; i.e., at large light-front momentum fractions x. This has important consequences for heavy quark production at large x_F, large p_T and at threshold; it also affects the weak decays of the B-meson [105]. The coupling $Q\bar{Q} \to H$ in the five-quark Fock state $|uudQ\bar{Q}>$ of the proton predicts Higgs production at large x_F at the LHC and LHeC.

2. The lensing effects of Initial-state and final-state Interactions are generally assumed to be higher-twist corrections; i.e., power-law suppressed. This is contradicted by diffractive deep-inelastic reactions and factorization-breaking phenomena such as the leading-twist Sivers effect in polarized single-inclusive deep inelastic scattering [15] and the breakdown [56] of the Lam-Tung relation for the angular distribution observed in the $\pi N \to \mu^+\mu^- X$ Drell-Yan reactions.

3. Structure functions are usually assumed to reflect the physics of the wavefunction of the hadron only, and thus they must be process independent. However, the observed structure functions are sensitive to process-dependent

rescattering and lensing processes at leading twist. One thus should distinguish "dynamical" versus "static" structure functions [21].

4. The antishadowing of the nuclear structure functions is conventionally assumed to be process-independent. In fact, each quark can have its own antishadowing distribution [22, 64], thus explaining the apparent absence of antishadowing in the NuTeV charged-current data [63].

5. High-transverse momentum hadrons in inclusive reactions are usually associated with quark or gluon jet fragmentation. In fact, high p_T hadrons can arise directly from a hard-twist subprocess such as $uu \to p\bar{u}$; since the directly produced hadrons are color-transparent, one can not only explain the observed power-law dependence of the fixed x_T cross section, but also the "baryon anomaly": the large baryon-to-meson ratio observed in heavy-ion collisions at RHIC [40].

6. It is usually argued that the renormalization scale in pQCD cannot be fixed at finite order and thus must be guessed or chosen to minimize sensitivity. In fact, the renormalization scale can be determined at each order in perturbation theory using the principle of maximal conformality(PMC) [68, 69] which absorbs all β-dependent nonconformal terms into the scale of the QCD coupling. The resulting predictions for physical observables are independent of the choice of the renormalization scheme. The PMC agrees with the conventional QED scale-setting procedure in the Abelian limit.

7. QCD "condensates" are conventionally assumed to be intrinsic properties of the physical vacuum. The conflict of this assumption with the observed cosmological constant highlights the need to distinguish different concepts of the vacuum: the acausal frame-dependent instant-form vacuum (the lowest energy state of the instant-form Hamiltonian) which must be normal-ordered, versus the causal frame-independent light-front definition [90]. Vacuum condensates are replaced by hadronic matrix elements in the Bethe-Salpeter and light-front analyses.

8. Nuclei are usually assumed to be composites of color-singlet nucleons; in fact, QCD also predicts "hidden color" configurations of the quarks; these components of the nuclear wavefunction may dominate the amplitude when evaluating short-distance nuclear reactions. [106]

9. The real part of the virtual Compton scattering amplitude is often regarded as an arbitrary subtraction term. However, the QCD LF Hamiltonian predicts an instantaneous four-point photon-quark interaction which is instantaneous in LF time. This leads to to a real contribution to the real and virtual Compton scattering amplitudes [107] – "a $J = 0$ fixed pole" contribution which is constant in energy and independent of the photons' virtuality at fixed momentum transfer.

10. Gluon degrees of freedom should be manifest at all scales - however, in AdS/QCD the effects of soft gluons are "sublimated" – absorbed in the QCD confinement potential [108].

11. Orbital angular momentum of the quarks and gluons in hadronic eigenstates is often assumed to be negligible. In fact, in AdS/QCD the nucleon eigensolutions for the light quarks have $L^z = \pm 1$ orbital angular momentum components comparable in strength to their $L^z = 0$ component [80]. This observation can explain observations showing that the nucleon's spin is largely carried by its constituents' angular momentum rather than their spin.

Acknowledgments

Presented at the International Workshop on Low-x Physics, 30 May - 04 Jun 2013, Eilat, Israel. I thank my collaborators for many helpful conversations. This research was supported by the Department of Energy contract DE–AC02–76SF00515. SLAC-PUB-15823.

[1] S. J. Brodsky, G. de Teramond and M. Karliner, Ann. Rev. Nucl. Part. Sci. **62**, 1 (2012) [arXiv:1302.5684 [hep-ph]].
[2] S. J. Brodsky and J. R. Primack, Annals Phys. **52**, 315 (1969).
[3] S. J. Brodsky, D. S. Hwang, B. -Q. Ma and I. Schmidt, Nucl. Phys. B **593**, 311 (2001) [hep-th/0003082].
[4] G. F. de Teramond and S. J. Brodsky, Phys. Rev. Lett. **102**, 081601 (2009) [arXiv:0809.4899 [hep-ph]].
[5] S. J. Brodsky, G. F. de Teramond and H. G. Dosch, arXiv:1302.4105 [hep-th].
[6] S. J. Brodsky, G. F. de Tramond and H. Gn. Dosch, arXiv:1309.4856 [hep-th].
[7] S. J. Brodsky, M. Diehl and D. S. Hwang, Nucl. Phys. B **596**, 99 (2001) [hep-ph/0009254].

[8] S. J. Brodsky, P. Hoyer, C. Peterson and N. Sakai, Phys. Lett. B **93**, 451 (1980).
[9] G. P. Lepage and S. J. Brodsky, Phys. Lett. B **87**, 359 (1979).
[10] G. P. Lepage and S. J. Brodsky, Phys. Rev. D **22**, 2157 (1980).
[11] A. V. Efremov and A. V. Radyushkin, Phys. Lett. B **94**, 245 (1980).
[12] E. L. Berger and S. J. Brodsky, Phys. Rev. Lett. **42**, 940 (1979).
[13] A. H. Mueller, Nucl. Phys. B **415**, 373 (1994).
[14] D. W. Sivers, Phys. Rev. D **41**, 83 (1990).
[15] S. J. Brodsky, D. S. Hwang and I. Schmidt, Phys. Lett. B **530**, 99 (2002) [hep-ph/0201296].
[16] J. C. Collins, Phys. Lett. B **536**, 43 (2002) [hep-ph/0204004].
[17] S. J. Brodsky, D. S. Hwang and I. Schmidt, Nucl. Phys. B **642**, 344 (2002) [hep-ph/0206259].
[18] S. J. Brodsky, D. S. Hwang, Y. V. Kovchegov, I. Schmidt and M. D. Sievert, Phys. Rev. D **88**, 014032 (2013) [arXiv:1304.5237 [hep-ph]].
[19] S. J. Brodsky, B. Pasquini, B. -W. Xiao and F. Yuan, Phys. Lett. B **687**, 327 (2010) [arXiv:1001.1163 [hep-ph]].
[20] S. J. Brodsky, P. Hoyer, N. Marchal, S. Peigne and F. Sannino, Phys. Rev. D **65**, 114025 (2002) [hep-ph/0104291].
[21] S. J. Brodsky, Nucl. Phys. A **827**, 327C (2009) [arXiv:0901.0781 [hep-ph]].
[22] S. J. Brodsky, I. Schmidt and J. -J. Yang, Phys. Rev. D **70**, 116003 (2004) [hep-ph/0409279].
[23] S. J. Brodsky and A. H. Mueller, Phys. Lett. B **206**, 685 (1988).
[24] S. J. Brodsky, C. -R. Ji and G. P. Lepage, Phys. Rev. Lett. **51**, 83 (1983).
[25] M. Franz, M. V. Polyakov and K. Goeke, Phys. Rev. D **62**, 074024 (2000) [hep-ph/0002240].
[26] S. J. Brodsky, G. F. de Teramond and R. Shrock, AIP Conf. Proc. **1056**, 3 (2008) [arXiv:0807.2484 [hep-ph]].
[27] A. Airapetian *et al.* [HERMES Collaboration], Phys. Lett. B **666**, 446 (2008) [arXiv:0803.2993 [hep-ex]].
[28] S. J. Brodsky, J. C. Collins, S. D. Ellis, J. F. Gunion and A. H. Mueller, DOE/ER/40048-21 P4.
[29] B. W. Harris, J. Smith and R. Vogt, Nucl. Phys. B **461**, 181 (1996) [hep-ph/9508403].
[30] W. -C. Chang and J. -C. Peng, Phys. Lett. B **704**, 197 (2011) [arXiv:1105.2381 [hep-ph]].
[31] G. Bari, M. Basile, G. Bruni, G. Cara Romeo, R. Casaccia, L. Cifarelli, F. Cindolo and A. Contin *et al.*, Nuovo Cim. A **104**, 1787 (1991).
[32] J. Pumplin, H. L. Lai and W. K. Tung, Phys. Rev. D **75**, 054029 (2007) [hep-ph/0701220].
[33] T. Stavreva, I. Schienbein, F. Arleo, K. Kovarik, F. Olness, J. Y. Yu and J. F. Owens, JHEP **1101**, 152 (2011) [arXiv:1012.1178 [hep-ph]].
[34] V. M. Abazov *et al.* [D0 Collaboration], Phys. Rev. Lett. **102**, 192002 (2009) [arXiv:0901.0739 [hep-ex]].
[35] J. Engelfried [SELEX Collaboration], Nucl. Phys. A **752**, 121 (2005).
[36] S. J. Brodsky, F. -K. Guo, C. Hanhart and U. -G. Meissner, Phys. Lett. B **698**, 251 (2011) [arXiv:1101.1983 [hep-ph]].
[37] S. J. Brodsky, B. Kopeliovich, I. Schmidt and J. Soffer, Phys. Rev. D **73**, 113005 (2006) [hep-ph/0603238].
[38] S. J. Brodsky, A. S. Goldhaber, B. Z. Kopeliovich and I. Schmidt, Nucl. Phys. B **807**, 334 (2009) [arXiv:0707.4658 [hep-ph]].
[39] D. W. Sivers, S. J. Brodsky and R. Blankenbecler, Phys. Rept. **23**, 1 (1976).
[40] F. Arleo, S. J. Brodsky, D. S. Hwang and A. M. Sickles, Phys. Rev. Lett. **105**, 062002 (2010) [arXiv:0911.4604 [hep-ph]].
[41] F. Arleo, S. J. Brodsky, D. S. Hwang and A. M. Sickles, arXiv:1006.4045 [hep-ph].
[42] S. J. Brodsky and A. Sickles, Phys. Lett. B **668**, 111 (2008) [arXiv:0804.4608 [hep-ph]].
[43] S. S. Adler *et al.* [PHENIX Collaboration], Phys. Rev. Lett. **91**, 172301 (2003) [nucl-ex/0305036].
[44] R. Blankenbecler, S. J. Brodsky and J. F. Gunion, eConf C **720906V1**, 504 (1972).
[45] E. M. Aitala *et al.* [E791 Collaboration], Phys. Rev. Lett. **86**, 4773 (2001) [hep-ex/0010044].
[46] J. Collins and J. -W. Qiu, Phys. Rev. D **75**, 114014 (2007) [arXiv:0705.2141 [hep-ph]].
[47] Z. Lu and I. Schmidt, Phys. Rev. D **75**, 073008 (2007) [hep-ph/0611158].
[48] A. Airapetian *et al.* [HERMES Collaboration], Phys. Rev. Lett. **94**, 012002 (2005) [hep-ex/0408013].
[49] F. Bradamante [COMPASS Collaboration], Nuovo Cim. C **035N2**, 107 (2012) [arXiv:1111.0869 [hep-ex]].
[50] M. G. Alekseev *et al.* [COMPASS Collaboration], Phys. Lett. B **692**, 240 (2010) [arXiv:1005.5609 [hep-ex]].
[51] F. Bradamante, Mod. Phys. Lett. A **24**, 3015 (2009).
[52] H. Avakian *et al.* [CLAS Collaboration], Phys. Rev. Lett. **105**, 262002 (2010) [arXiv:1003.4549 [hep-ex]].
[53] H. Gao, L. Gamberg, J. P. Chen, X. Qian, Y. Qiang, M. Huang, A. Afanasev and M. Anselmino *et al.*, Eur. Phys. J. Plus **126**, 2 (2011) [arXiv:1009.3803 [hep-ph]].
[54] S. Falciano *et al.* [NA10 Collaboration], Z. Phys. C **31**, 513 (1986).
[55] C. S. Lam and W. -K. Tung, Phys. Rev. D **21**, 2712 (1980).
[56] D. Boer, S. J. Brodsky and D. S. Hwang, Phys. Rev. D **67**, 054003 (2003) [hep-ph/0211110].
[57] D. Boer, Phys. Rev. D **60**, 014012 (1999) [hep-ph/9902255].
[58] Z. -t. Liang and T. -c. Meng, Phys. Rev. D **49**, 3759 (1994).
[59] C. Adloff *et al.* [H1 Collaboration], Z. Phys. C **76**, 613 (1997) [hep-ex/9708016].
[60] J. Breitweg *et al.* [ZEUS Collaboration], Eur. Phys. J. C **6**, 43 (1999) [hep-ex/9807010].
[61] L. Stodolsky, Phys. Lett. B **325**, 505 (1994).
[62] S. J. Brodsky, AIP Conf. Proc. **1105**, 315 (2009) [arXiv:0811.0875 [hep-ph]].
[63] I. Schienbein, J. Y. Yu, C. Keppel, J. G. Morfin, F. I. Olness and J. F. Owens, arXiv:0806.0723 [hep-ph].
[64] S. J. Brodsky and H. J. Lu, Phys. Rev. Lett. **64**, 1342 (1990).
[65] A. V. Belitsky, X. Ji and F. Yuan, Nucl. Phys. B **656**, 165 (2003) [hep-ph/0208038].
[66] J. C. Collins and A. Metz, Phys. Rev. Lett. **93**, 252001 (2004) [hep-ph/0408249].

[67] G. Kramer and B. Lampe, Z. Phys. C **39**, 101 (1988).
[68] S. J. Brodsky and L. Di Giustino, Phys. Rev. D **86**, 085026 (2012) [arXiv:1107.0338 [hep-ph]].
[69] S. J. Brodsky and X. -G. Wu, Phys. Rev. D **85**, 034038 (2012) [Erratum-ibid. D **86**, 079903 (2012)] [arXiv:1111.6175 [hep-ph]].
[70] M. Mojaza, S. J. Brodsky and X. -G. Wu, Phys. Rev. Lett. **110**, 192001 (2013) [arXiv:1212.0049 [hep-ph]].
[71] S. J. Brodsky, G. P. Lepage and P. B. Mackenzie, Phys. Rev. D **28**, 228 (1983).
[72] S. J. Brodsky, M. Mojaza and X. -G. Wu, arXiv:1304.4631 [hep-ph].
[73] S. J. Brodsky and X. -G. Wu, Phys. Rev. D **85**, 114040 (2012) [arXiv:1205.1232 [hep-ph]].
[74] S. J. Brodsky and H. J. Lu, Phys. Rev. D **51**, 3652 (1995) [hep-ph/9405218].
[75] S. J. Brodsky, G. T. Gabadadze, A. L. Kataev and H. J. Lu, Phys. Lett. B **372**, 133 (1996) [hep-ph/9512367].
[76] X. -G. Wu, S. J. Brodsky and M. Mojaza, Prog. Part. Nucl. Phys. **72**, 44 (2013) [arXiv:1302.0599 [hep-ph]].
[77] S. J. Brodsky, E. Gardi, G. Grunberg and J. Rathsman, Phys. Rev. D **63**, 094017 (2001) [hep-ph/0002065].
[78] J. M. Maldacena, Adv. Theor. Math. Phys. **2**, 231 (1998) [hep-th/9711200].
[79] G. F. de Teramond and S. J. Brodsky, Nucl. Phys. Proc. Suppl. **199**, 89 (2010) [arXiv:0909.3900 [hep-ph]].
[80] S. J. Brodsky and G. F. de Teramond, AIP Conf. Proc. **1388**, 22 (2011) [arXiv:1103.1186 [hep-ph]].
[81] S. J. Brodsky, G. F. de Teramond and A. Deur, Phys. Rev. D **81**, 096010 (2010) [arXiv:1002.3948 [hep-ph]].
[82] S. S. Chabysheva and J. R. Hiller, Few Body Syst. **52**, 323 (2012) [arXiv:1110.5324 [hep-ph]].
[83] T. Branz, T. Gutsche, V. E. Lyubovitskij, I. Schmidt and A. Vega, Phys. Rev. D **82**, 074022 (2010) [arXiv:1008.0268 [hep-ph]].
[84] S. J. Brodsky, G. F. de Teramond and H. G. Dosch, arXiv:1302.4105 [hep-th].
[85] V. de Alfaro, S. Fubini and G. Furlan, Nuovo Cim. A **34**, 569 (1976).
[86] G. F. de Teramond, H. G. Dosch and S. J. Brodsky, Phys. Rev. D **87**, 075005 (2013) [arXiv:1301.1651 [hep-ph]].
[87] A. Zee, Mod. Phys. Lett. A **23**, 1336 (2008).
[88] S. Weinberg, Phys. Rev. Lett. **59**, 2607 (1987).
[89] S. J. Brodsky and R. Shrock, Proc. Nat. Acad. Sci. **108**, 45 (2011) [arXiv:0803.2554 [hep-th]]. [arXiv:0905.1151 [hep-th]].
[90] S. J. Brodsky, C. D. Roberts, R. Shrock and P. C. Tandy, Phys. Rev. C **82**, 022201 (2010) [arXiv:1005.4610 [nucl-th]].
[91] S. J. Brodsky, C. D. Roberts, R. Shrock and P. C. Tandy, Phys. Rev. C **85**, 065202 (2012) [arXiv:1202.2376 [nucl-th]].
[92] P. A. M. Dirac, Rev. Mod. Phys. **21**, 392 (1949).
[93] P. P. Srivastava and S. J. Brodsky, Phys. Rev. D **66**, 045019 (2002) [hep-ph/0202141].
[94] S. J. Brodsky and R. Shrock, Phys. Lett. B **666**, 95 (2008) [arXiv:0806.1535 [hep-th]].
[95] A. Casher and L. Susskind, Phys. Rev. D **9**, 436 (1974).
[96] M. Burkardt, In *Seoul 1997, QCD, lightcone physics and hadron phenomenology* 170-199 [hep-ph/9709421].
[97] P. Maris, C. D. Roberts and P. C. Tandy, Phys. Lett. B **420**, 267 (1998) [nucl-th/9707003].
[98] P. Maris and C. D. Roberts, Phys. Rev. C **56**, 3369 (1997) [nucl-th/9708029].
[99] L. Chang, C. D. Roberts and D. J. Wilson, arXiv:1201.3918 [nucl-th].
[100] L. Chang, C. D. Roberts and P. C. Tandy, Phys. Rev. C **85**, 012201 (2012) [arXiv:1109.2903 [nucl-th]].
[101] L. Chang and C. D. Roberts, AIP Conf. Proc. **1361**, 91 (2011) [arXiv:1003.5006 [nucl-th]].
[102] B. L. Ioffe and K. N. Zyablyuk, Eur. Phys. J. C **27**, 229 (2003) [hep-ph/0207183].
[103] M. Davier, A. Hocker and Z. Zhang, Nucl. Phys. Proc. Suppl. **169**, 22 (2007) [hep-ph/0701170].
[104] M. Davier, S. Descotes-Genon, A. Hocker, B. Malaescu and Z. Zhang, Eur. Phys. J. C **56**, 305 (2008) [arXiv:0803.0979 [hep-ph]].
[105] S. J. Brodsky and S. Gardner, Phys. Rev. D **65**, 054016 (2002) [hep-ph/0108121].
[106] C. -R. Ji and S. J. Brodsky, Phys. Rev. D **34**, 1460 (1986).
[107] S. J. Brodsky, F. J. Llanes-Estrada and A. P. Szczepaniak, Phys. Rev. D **79**, 033012 (2009) [arXiv:0812.0395 [hep-ph]].
[108] S. J. Brodsky and G. F. de Teramond, PoS QCD **-TNT-II**, 008 (2011) [arXiv:1112.4212 [hep-th]].